City Research Online

City St George's, University of London

Citation: Mian, A. & Reyes-Aldasoro, C. C. (2015). Quantification of the Effects of Low Dose Radiation and its Impact on Cardiovascular Risks. Paper presented at the Quantification of the Effects of Low Dose Radiation and its Impact on Cardiovascular Risks.

This is the accepted version of the paper.

This version of the publication may differ from the final published version. To cite this item please consult the publisher's version.

Permanent repository link: https://openaccess.city.ac.uk/id/eprint/11966/

Copyright and Reuse: Copyright and Moral Rights remain with the author(s) and/or copyright holders. Copies of full items can be used for personal research or study, educational, or not-for-profit purposes without prior permission or charge, unless otherwise indicated, provided that the authors, title and full bibliographic details are credited, a hyperlink and/or URL is given for the original metadata page and the content is not changed in any way. For full details of reuse please refer to City Research Online policy.

City Research Online: http://openaccess.city.ac.uk/ publications@citystgeorges.ac.uk

Quantification of the Effects of Low Dose Radiation and its Impact on Cardiovascular Risks

Atif S. Mian [1]
Atif.mian.1@city.ac.uk
C.C Reyes-Aldasoro[1]
reyes@city.ac.uk
http://staff.city.ac.uk/~sbbk034/

[1] School of Mathematics, Computer Science and Engineering, City University London, EC1V 0HB, UK

Abstract

This work describes an algorithm developed to quantify the effects of low dose radiation on the cardiac endothelial cells with the final objective of inferring how radiation may potentially initiate cardiovascular disease in post radiotherapy-treated patients. The effects are investigated by using an *in-vitro* co-culture cellular matrix, consisting of endothelial cells on a base of fibroblasts, which in time begin to form capillary (tubular) like structures. A range of radiation doses (0.2-16 Gray (Gy)) was applied to different samples and the effects observed. The automatic segmentation is validated against a set of manual segmented images with satisfactory results presenting a correct classification of 0.93; classification is the measure of comparison between two sets of images, specified as a number from 0 to 1, whereby 1 denotes 100% similarity whilst 0 refers to 0% similarity. Measurements related to geometrical parameters were further obtained. It was found during the course of this project, the largest observable change in endothelial cell structure was found after exposure to 0.2 Grays of radiation.

1 Introduction

In the United Kingdom an estimated number of ≥ 331,000 people were diagnosed with cancer in 2011. Of this number, approximately two-thirds receive radiotherapy as a treatment [1]. Patients receiving Mediastinal (chest) radiotherapy for treatment of Breast cancer, Lung cancer, Oesophageal cancer and Hodgkin's lymphoma are at the highest risk of exposing ionising radiation to the heart [2].

The heart has long been considered one of the few organs to be moderately resistant to radiation induced tissue damage [3]. However, recent epidemiological studies propose evidence to the contrary [4]. So far, current epidemiological statistics have revealed that moderate to low doses of radiation to the heart may possibly result in a substantial increase in cardiovascular associated mortality [5]. Though, the pathogenesis of heart disease from irradiation, as of yet, has not been explored in detail.

There are various techniques used to quantify the effects of radiation. One of these methods consists of irradiating cardiac cells *in-vitro* and subsequently assessing the effects

© 2015. The copyright of this document resides with its authors.
It may be distributed unchanged freely in print or electronic forms.

of the radiation on the morphological and functional properties of cardiomyocytes and endothelial cells; the cells that form thin layers that cover the inner part of blood vessels [6][7]. Endothelial cells in a co-culture system contained by fibroblasts develop with time, eventually forming tube-like structures similar in appearance to capillaries. Such a system is used in accordance to replicate the *in-vivo* angiogenic process; hence, it can be used to test inhibitors and activators of angiogenesis [8].

The aim of this work is to investigate the effects of ionising radiation on the cardiac endothelial cells (microvasculature) grown *in-vitro* and its relation to angiogenesis inhibition. Tube/capillary-like structures are formed in a perfusion (live) co-culture system consisting of endothelial cells and fibroblasts derived from Murinae heart cells. These cells are subjected to various levels of ionising radiation (0, 0.2, 2, 8, and 16 Gy) [n=5×3]; 0 Gy acting as the reference control for this research. Images of the Murinae heart cells were acquired twenty weeks post irradiation. A sequence of segmentation and geometric analysis algorithms will be performed on the obtained co-cultured Murinae heart cell images via MATLAB programming. These algorithms will subsequently allow observational measurements of dosage effects in correlation to time after radiation.

2 Materials and Methods

2.1 Materials

Organotypic cultures (the process of growing cells in a 3-D environment, producing a cellular system that is biochemically and physiologically more resembling in nature to *in-vivo* tissue as opposed to 2-D culture sets) were stained with lectin to identify the endothelial cells and a representative image at each irradiation dose is shown in Fig. 1. The images are greyscale and with low contrast, and each comprises a cluttered background overlaid with the tube-like structures formed by endothelial cells. There are significant inter-image and intra-image illumination variations. Dead cells or debris were also present, sometimes occluding the tubules. The tubules are the primary target of the analysis (as changes of these structures indicate the progression of angiogenesis), though the debris; biological in nature rather than imaging artefacts, is also relevant.

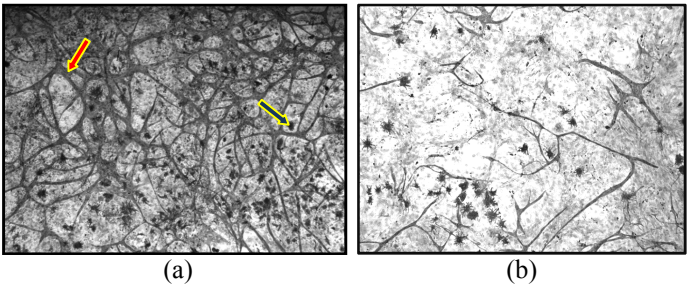

(a) (b)

Figure 1: Two representative images. (a) An image of a 0 Gy (control) cultured murinae heart cell. The debris is highlighted by the blue arrow (right), whilst the tubules are highlighted by the red arrow (left). See how brightness increases from the top of the image down to the bottom. A simple thresholding technique would leave the top relatively dark compared to the bottom, which would cause some of the tubules to be classed as background. (b) Image treated with 8 Gy; notice the difference in density and intensity of the background.

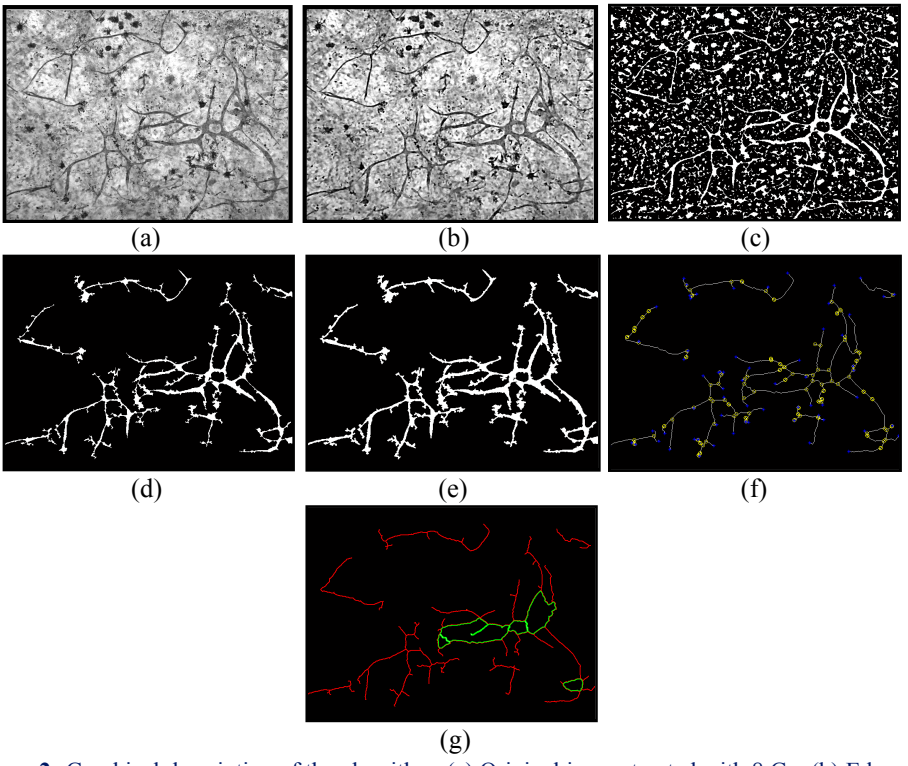

Figure 2: Graphical description of the algorithm. (a) Original image treated with 8 Gy. (b) Edges are highlighted with the application of 3×3 median filter and un-sharp filter. (c) Binarisation with adaptive thresholding (window size = 35, mean-C = 0.02) and erosion with a disk structural element was applied. (d) Objects smaller than 350 pixels in diameter were removed with morphological operators. (e) Gaps closed by dilation with a disk structural element. (f) Skeleton, branch (yellow-dots) and end points (blue dots). (g) The final step was to detect closed meshes (green) as it was assumed the number of meshes to be related with the health of the cellular development.

2.2 Algorithm description

The steps of the algorithm were programmed in MATLAB and the image processing toolbox. These algorithms were designed to assist in separating the relevant elements of the data, i.e., the structure of the tubules, their density per area, size, length and also the geometric distribution; through identification of the number of tubules that go onto form junctions, ones that are isolated within the matrix and furthermore, finding their relative branching angles.

Several challenges for the segmentation process were identified. Since majority of the images exhibit low contrast, they become extremely difficult to differentiate from the surrounding information, especially at the edges. For this reason, simple segmentation based on intensity was not suitable due to the low contrast exhibited by the tubules. By eliminating unnecessary shading [9], the images will gain a more uniform background intensity. Thus, alternative segmentation techniques can be applied to facilitate the analysis of the individual structures and their characteristics, by dividing the image into three distinct components; the debris, background and tube/capillary like structures. Prior to performing automatic segmentation, all data sets were manually segmented by a single

user to create a gold standard for comparison purposes [n=5×3]. The gold standard set was achieved through collectively adding successive masks of the individual tube like structures of each image using the MATLAB function *roipoly*.

In order to quantify the angiogenic process, the following steps were performed; segmenting the background and debris from the tubules, skeletonising the tubules and from them, determining the branch and end points of the structure, the number of meshes and mesh area (Fig. 2). All these help in quantifying the vessel structure.

3 Results

Classification of the results was achieved by subtracting the automatic segmented images from its equivalent manual set. From the results an average correct classification of 0.93 was obtained, the lowest being 0.85 and the highest being 0.97 (Fig. 3), which are similar to those reported in [5]. The main benefit of the automatic segmentation is time efficiency. Manual segmentation of 15 required approximately 3-4 hours per image, depending on the complexity of the tubules. The automatic segmentation on the other hand took only seconds. However, there is a trade-off between accuracy and time efficiency using automatic segmentation over manual segmentation.

The automatic algorithm found a lower number of meshes as compared to the gold standard, (Fig.4).The number of closed meshes were considered to be one important feature of the angiogenic process. An average reduction of 23% in the number of meshes was observed. This is partly attributed to some of the tubule structures being deleted during the morphological erosion phase necessary to remove the debris. Nonetheless, by applying a suitable dilation phase, some of the mesh structures could be restored.

When quantifying the manual set images, an inverse relationship to the radiation dose was witnessed. This trend may be related to the suppression of the signalling protein, vascular endothelial growth factor (VEGF). It has been reported [10] that an increase in ionising radiation reduces the levels of VEGF and its receptor VEGFR-2, which are pivotal in the role of endothelial cell proliferation, hence, a reduction in blood vessel formation. It is interesting to see, from the results below, that the most drastic angiogenic inhibition occurs between 0 and 0.2 Gy whereby a ~20% decrease in mesh area is noticed. This may indicate a prominent rise in VEGF suppression must occur after initial exposure to low range doses of ionising radiation, therefore resulting in the changes recognized [5]. The MATLAB function ‘Spy’ was used to identify the number of meshes within the vessel matrix. This function also produced an adjacency matrix that showed the number of meshes that are neighbouring each other. From this it was found, as the radiation dosage increased so did the distance between the mesh structures within the co-culture system.

A linear regression analysis was carried out in MATLAB (statistics toolbox) to see the relationship between automatic segmented branch points and manual segmented branch points and also their equivalent mesh area. An R-squared value of 0.90 (for branch points) and 0.81 (for mesh area) was observed ($P < 0.05$). This shows that the regression line fits the data fairly well, suggesting that there is very little difference in the classification between automatic and manual segmentation, thus, owing potential for automatic segmentation to gain precedence over manual segmentation in practise, as it produces high classification, whilst also offering a considerable reduction in time consumed (greater efficiency), therefore, can be used to dose-determine multiple sets of images in relatively short periods of time.

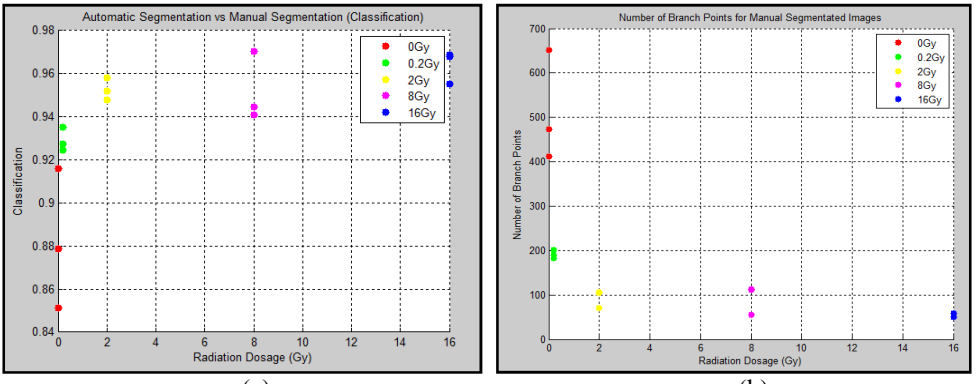

(a) (b)

Figure 3: (a) Comparison of manual and automatic classifications against radiation dosage. Correct classification rose amid increase in radiation. It is assumed that as the tubule density decreased, the background had a higher weight in the classification. (b) Number of branch points vs. Radiation dosage. The number of branch points decreased with higher radiation doses.

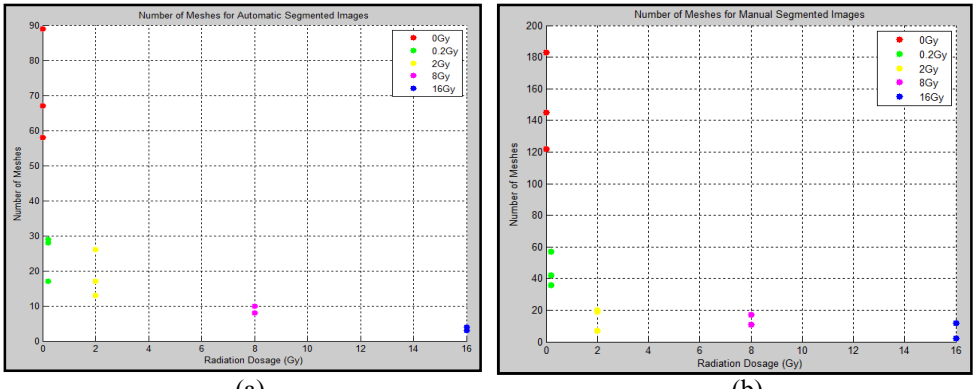

(a) (b)

Figure 4: Comparison of number of meshes detected for (a) automatic and (b) manual segmentations. It is clear that fewer meshes were detected with the automatic segmentation.

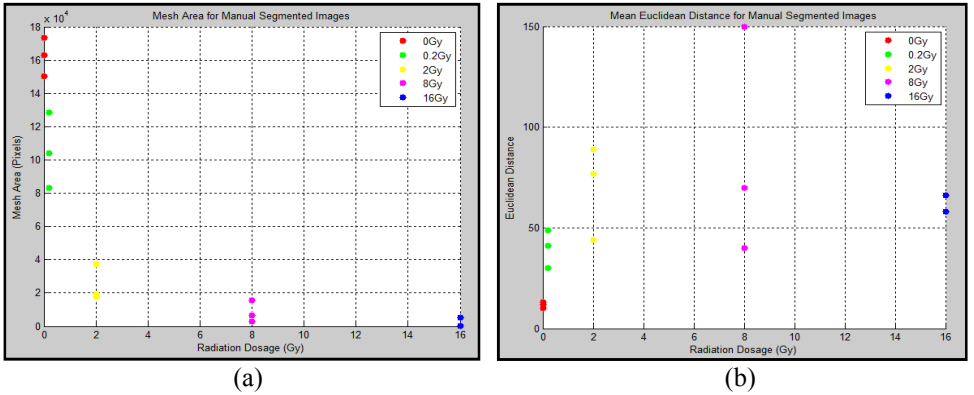

(a) (b)

Figure 5: (a) Mesh area and (b) Euclidean distance against radiation dosage. Notice the reduction of the mesh area with higher doses. However, the Euclidean distance did not show any correlation.

4 Conclusion

This work presented a segmentation algorithm for the analysis of the effects of irradiation in *in-vitro* cardiac cells. The algorithm was programmed in Matlab and followed several steps: adaptive thresholding, morphological erosion in conjunction with morphological operators for artefact removal. The average correct classification against the manual segmentation was 0.93. Whilst sequentially reviewing the data, it was noted that lowest dosage of radiation produced the greatest structural change in the tubular structure; suggesting even low doses of radiation exhibit high angiogenic inhibition. Automatic segmentation yielded fairly robust results and may possibly be used for identification and quantification of blood vessel changes *in-vitro* in place of manual segmentation. In the future we can analyse other metrics like Jaccard score and more sophisticated processing like separation into training and testing sets.

References

[1] C. R. UK, "Cancer Stats: Key Stats," 02-Apr-2015. [Online]. Available: http://www.cancerresearchuk.org/cancer-info/cancerstats/keyfacts/cancerstats-key-facts-on-cancer. [Accessed: 01-May-2015].

[2] M. J. Adams, P. H. Hardenbergh, L. S. Constine, and S. E. Lipshultz, "Radiation-associated cardiovascular disease," *Crit. Rev. Oncol. Hematol.*, vol. 45, no. 1, pp. 55–75, Jan. 2003.

[3] S. W. Yusuf, S. Sami, and I. N. Daher, "Radiation-Induced Heart Disease: A Clinical Update," *Cardiol. Res. Pract.*, vol. 2011, p. e317659, Feb. 2011.

[4] L. Cella, J. H. Oh, J. O. Deasy, G. Palma, R. Liuzzi, V. D'avino, M. Conson, M. Picardi, M. Salvatore, and R. Pacelli, "Predicting radiation-induced valvular heart damage," *ActaOncol. Stockh. Swed.*, pp. 1–9, Mar. 2015.

[5] S. Bowyer, C. Kanthou, and C. C. Reyes-Aldasoro, "Analysis of capillary-like structures formed by endothelial cells in a novel organotypic assay developed from heart tissue.," presented at the Medical Image Understanding and Analysis, London, UK, 2014, pp. 235–240.

[6] G. M. Tozer, S. Akerman, N. A. Cross, P. R. Barber, M. A. Björndahl, O. Greco, S. Harris, S. A. Hill, D. J. Honess, C. R. Ireson, K. L. Pettyjohn, V. E. Prise, C. C. Reyes-Aldasoro, C. Ruhrberg, D. T. Shima, and C. Kanthou, 'Blood vessel maturation and response to vascular-disrupting therapy in single vascular endothelial growth factor-A isoform-producing tumors', *Cancer Res.*, vol. 68, no. 7, pp. 2301–2311, Apr. 2008.

[7] "CARDIORISK." [Online]. Available: http://www.cardiorisk.eu. [Accessed: 01-May-2015].

[8] C. C. Reyes-Aldasoro, D. Biram, G. M. Tozer, and C. Kanthou, 'Measuring cellular migration with image processing', *Electron. Lett.*, vol. 44, no. 13, pp. 791–793, Jun. 2008.

[9] C. C. Reyes-Aldasoro, "Retrospective shading correction algorithm based on signal envelope estimation," *Electron. Lett.*, vol. 45, no. 9, p. 454, 2009.

[10] J. Li, S. Huang, E. A. Armstrong, J. F. Fowler, and P. M. Harari, "Angiogenesis and radiation response modulation after vascular endothelial growth factor receptor-2 (VEGFR2) blockade," *Int. J. Radiat. Oncol. Biol. Phys.*, vol. 62, no. 5, pp. 1477–1485, Aug. 2005.